

Fluorinated and Charged Hydrogenated Alkanethiolates grafted on Gold: Expanding the Diversity of Mixed-Monolayer Nanoparticles for Biological Applications

Silvia Bidoggia,[†] Francesca Milocco,[†] Stefano Polizzi,[‡] Patrizia Canton,[‡] Alessandra Saccani,[§] Barbara Sanavio,[§] Silke Krol,[§] Francesco Stellacci,^{||,§} Paolo Pengo,^{*,†} Lucia Pasquato^{*,†}

[†]*Department of Chemical and Pharmaceutical Sciences, University of Trieste and INSTM Trieste Unit, via L. Giorgieri 1, 34127 Trieste, Italy;* [‡]*Dipartimento di Scienze Molecolari e Nanosistemi and Centro di Microscopia Elettronica R. Stevanato, Università Ca' Foscari Venezia, Via Torino 155/b, I-30172 Venezia-Mestre, Italy;* [§]*NanoMed lab, Fondazione IRCCS, Istituto Neurologico "Carlo Besta", IFOM-IEO-campus, via Adamello, Milan, Italy;* ^{||}*Institute of Materials, École Polytechnique Fédérale de Lausanne, Lausanne CH-1015, Switzerland.*

Abstract

Low intrinsic toxicity, high solubility and stability are important and necessary features of gold nanoparticles to be used in the bio-medical field. In this context, charged nanoparticles proved to be very versatile and among them charged mixed-monolayer gold nanoparticles, displaying monolayers with well-defined morphologies, represent a paradigm. By using mixtures of hydrogenated and fluorinated thiols, the formation of monolayer domains may be brought to an extreme because of the immiscibility of fluorinated and hydrogenated chains. Following this rationale, mixed monolayer gold nanoparticles featuring ammonium, sulfonate or carboxylic groups on their surface were prepared by using amphiphilic hydrogenated thiols and 1*H*,1*H*,2*H*,2*H*-perfluoro-alkanethiols. The toxicity of these systems was assessed in HeLa cells and was found to be, in general, low even for the cationic nanoparticles which usually show a high cytotoxicity and is comparable to that of homoligand gold nanoparticles displaying amphiphilic – charge neutral – hydrogenated or fluorinated thiolates in their monolayer. These properties make the mixed ligand monolayer gold nanoparticles an interesting new candidate for medical application.

Introduction

The unique lipophobic *and* hydrophobic nature of fluorocompounds represents a tremendous, but so far little exploited, opportunity in the design of self-assembled materials. Indeed, the use of fluorinated (F-) sub-units often yields species with very different structures and properties respect to hydrogenated (H-) analogues, offering a simple way to expand the diversity of systems for applications in the biomedical field. In this context, the extreme hydrophobicity of fluorocompounds may enable mechanisms of interaction with biologically relevant structures, such as cell membranes, that are different from those operative for hydrogenated systems. In addition, their stability, due to the strength of the C-F bonds, and low toxicity may also allow developing safe devices with extended lifetime *in vivo*. Several examples highlight the remarkable properties of nanosized fluorinated systems that hold promise of improving the efficacy of nanomedicine. For instance, decoration of gold nanoparticles (AuNPs) with short perfluoroether moieties¹ allowed their spontaneous self-assembly – triggered by fluorophilic interactions – into hollow superstructures² in the absence of external templates. A similar behavior was never reported for nanoparticles (NPs) bearing solely polyether units in their outermost layer. These NPs vesicles could be loaded with the fluorescent dye rhodamine or with the anticancer drug doxorubicin; this payload could then be released by laser irradiation at 532 nm,³ presenting potentialities as a drug delivery systems based on AuNPs.^{4,5} Soft NPs made of peptide nucleic acid (PNA) conjugated to perfluoroundecanoyl chains display a threefold higher cellular uptake by HeLa cells respect to undecanoyl PNA.⁶ Soft NPs obtained by complexation of polyampholites with perfluorododecanoic acid were found to hinder the formation of amyloid fibrils, while hydrogenated analogues were not effective.^{7,8} Furthermore, in a thermodynamic analysis of water soluble fluorinated AuNPs as putative drug delivery systems, we found that nanoparticles displaying fluorinated ligands on their surface interact with drug-like guests with higher affinity than hydrogenated NPs of similar structure.⁹ Fluorinated soft NPs have been, indeed, proposed as drug delivery systems for doxorubicin.^{10,11} An additional feature of fluorinated materials, including AuNPs, is that they may be easily engineered into contrast agents for ¹⁹F magnetic resonance imaging^{12,13} and by combining this application with drug delivery, novel theranostic platforms may become available.¹¹ As far as monolayer protected AuNPs are concerned, the immiscibility of F- and H-thiolate ligands, arising from the lipophobicity of fluorocompounds, favors their self-sorting, with formation of domains, on the NPs surface.¹⁴⁻¹⁶ This finding is in keeping with what observed in many examples of self-assembled systems comprising mixtures of hydrogenated and fluorinated components. For example, formation of phase segregated domains were indeed observed in the case of liposomes¹⁷ even when mixtures containing a mere 5% of fluorinated amphiphiles were used. The same behaviour was also

observed by AFM in supported lipid bilayer of 1,2-dipalmitoyl-*sn*-glycero-3-phosphocholine and of a semi-fluorinated analogue¹⁸ or in mixtures of Arachidic and partially fluorinated carboxylic acids.¹⁹ On the other hand, studies on mixed hydrogenated/fluorinated self-assembled monolayers (SAMs) on flat surfaces are suggestive of less facile phase segregation. In particular, the adsorption on Au(111) of mixed disulfides featuring a hydrogenated chain and a fluorinated chain of different lengths - in a single disulfide molecule - results in the formation of SAMs with no evidence of phase segregation.^{20,21} Occurrence of phase segregation was not observed even after thermal annealing.²² Interestingly, co-adsorption of a mixture of H- and F-thiols of the same length produces SAMs that are indistinguishable from the SAMs obtained by using the corresponding mixed disulfide.²⁰ Instead, adsorption of blends of dissimilar H- and F-thiols, results in the formation of small islands of the fluorinated ligands.²³

The self-sorting of hydrogenated and fluorinated thiolates on curved surfaces may be the basis for the preparation of spontaneously patterned monolayers and provides a further approach to control the morphology of mixed monolayers in addition to those unraveled by the experimental and theoretical analyses of Stellacci^{24,25} and Glotzer.^{26,27} In the context of nanoparticles-cell interaction, aside from the surface charge^{28,29} and functionalization,^{30,31} the morphology of the coating monolayer is pivotal in determining the efficiency and the mechanism of the internalization process;³²⁻³⁴ the latter being also responsible for the toxicity of the NPs.³⁵ This body of evidences comes from thorough analyses of mixed monolayer hydrogenated charged NPs of well-defined morphologies,³² while the effect of including F-ligands in the monolayer of these charged systems is, at present, completely unexplored. No information is also available on their toxicity in comparison to similar charged hydrogenated NPs. To start filling this gap, we then embarked in the synthesis of charged H-/F-mixed-monolayer AuNPs by using blends of thiols in which one of the components is a charged amphiphilic H-thiol while the F-component is selected among the readily available *1H,1H,2H,2H*-perfluoro-alkanethiols. In particular, in order to favor the solubility in aqueous solutions the F-thiols length has to be shorter than that of H-thiols but presenting at least six F-methylene groups in order to exploit the lipophobicity properties for the monolayer organization.¹⁵ These NPs systems display good solubility in polar media, including water. Their toxicity and internalization pathway were preliminarily assessed on HeLa cells.

Results and Discussion

For this study we prepared a series of H-/F- mixed monolayer AuNPs with different surface charge by using a mixture of ligands as reported in Figure 1A. The sodium salts of the 11-mercaptoundecanesulfonic acid (**HMUS**) and 12-mercaptododecanesulfonic acid (**HMDDS**) were

used to provide NPs with permanent negative charges. The 12-mercaptododecanoic acid (**HMDA**) was used to provide the NPs with ionizable groups on the surface while 12-mercapto-*N,N,N*-trimethyl-1-dodecanaminium chloride (**HTMDA**) was designed in order to obtain NPs featuring permanent positive charges. These thiols were used in combination with 1*H*,1*H*,2*H*,2*H*-perfluoro-1-decanethiol (**HF8**) or 1*H*,1*H*,2*H*,2*H*-perfluoro-1-octanethiol (**HF6**) as the fluorinated components. The uptake by HeLa cells and the cytotoxicity of these charged H-/F- mixed monolayer AuNPs were compared to those of charge neutral NPs obtained by using the thiols *N*-1-{2-[2-(2-methoxyethoxy)ethoxy]ethyl}-8-sulfanyloctanamide (**HC8TEG**) and 2,2,3,3,4,4,5,5,6,6,7,7,8,8,9,9-Hexadecafluoro-10-(methoxy-PEG550)decan-1-thiol (**HF8PEG**), Figure 1B. The synthesis of the thiols **HMDDS**, **HMDA** and **HTMDA** is reported in the Supporting Information (SI).

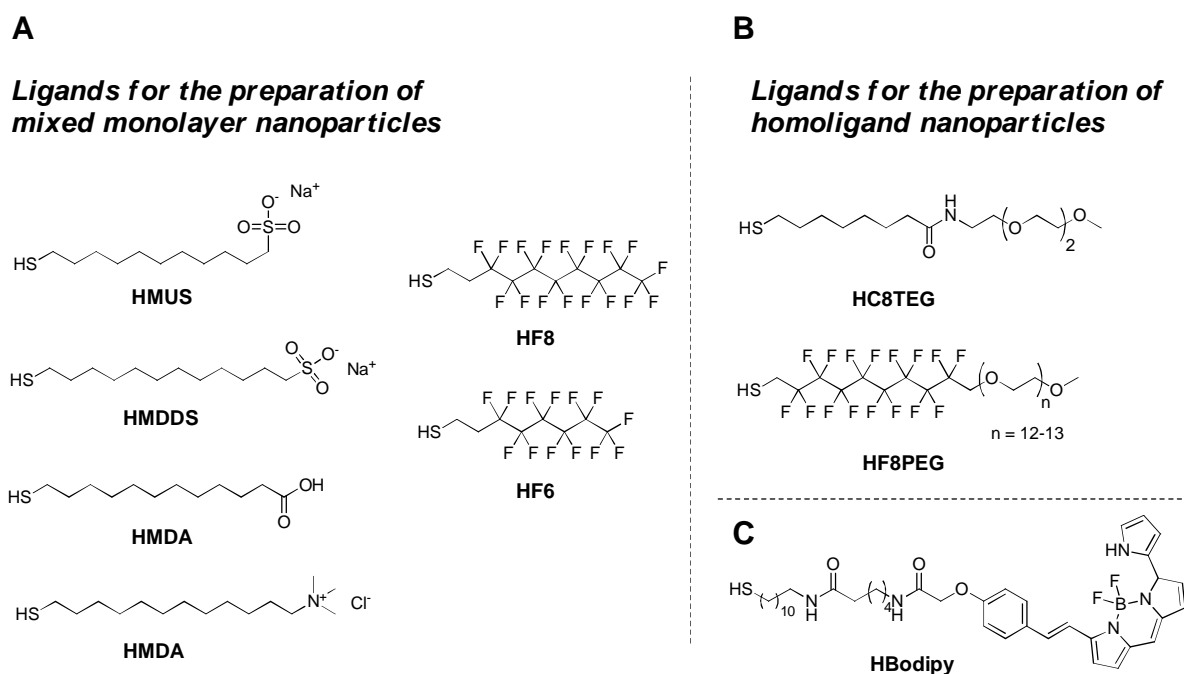


Figure 1. Thiols used in the preparation of charged H-/F-mixed-monolayer NPs, panel A; thiols used for the preparation of charge neutral homoligand AuNPs, panel B; and for NPs labeling, panel C.

Nanoparticles synthesis and characterization. The development of anionic H-/F- mixed monolayer NPs was attempted at first by using the hydrophilic thiols **HMUS** or **HMDDS** blended to the highly hydrophobic thiol **HF8** in a 2:1 molar ratio while the gold to thiols ratio was set to 1:1; the preparations were achieved by direct synthesis following the procedure reported by Stellacci and co-workers.³⁶ The obtained nanoparticles **NP-MUS/F8**³⁷ and **NP-MDDS/F8** were essentially insoluble in water. In seeking an improvement of the system solubility, the F-ligand in the blend was replaced by the shorter thiol **HF6** and this was used in combination with **HMDDS**, in order to ensure a better masking of the fluorinated thiolate and/or, of the fluorinated domains, from the solvent. The initial gold to thiols ratio was set to 2:1, in keeping with the previous cases, while the

HMDDS:HF6 ratio was set to 2:1.3 and the reducing agent was added dropwise over 15 minutes. The nanoparticles **NP-MDDS/F6-a** thus obtained displayed an average core diameter of 3.3 ± 0.5 nm, while, interestingly, the molar ratio between the **MDDS** and **F6** thiulates in the monolayer was close to 5:1, very different from the initial **HMDDS:HF6** ratio, Table 1, indicating that the introduction of thiolate **F6** in the monolayer of nanoparticles **NP-MDDS/F6-a** is a disfavored process.^{38,39}

Table 1. Characterization data for the nanoparticles used in this study.

Sample	initial H ^a : F6	x_{in}^F	Final H: F6 ^b	x_{fin}^F	Diameter, nm ^c	Nanoparticles Composition ^d
NP-MDDS/F6-a	1 : 0.65	0.40	5.0 : 1	0.17	3.3 ± 0.5	Au ₁₁₅₀ (MDDS) ₁₄₅ (F6) ₂₉
NP-MDDS/F6-b	1 : 0.77	0.44	2.5 : 1	0.29	3.2 ± 0.7	Au ₁₂₈₉ (MDDS) ₁₅₀ (F6) ₆₀
NP-MDDS/F6-c	1 : 0.90	0.47	1.5 : 1	0.40	3.4 ± 0.7	Au ₁₄₁₅ (MDDS) ₁₂₉ (F6) ₈₇
NP-MDA/F6-a	1 : 0.65	0.4	5.0 : 1	0.17	3.0 ± 0.5	Au ₉₇₆ (MDA) ₁₃₆ (F6) ₂₈
NP-MDA/F6-b	1 : 0.77	0.44	2.9 : 1	0.26	2.5 ± 0.6	Au ₅₂₃ (MDA) ₉₀ (F6) ₃₀
NP-MDA/F6-c	1 : 1.30	0.57	1.5 : 1	0.40	2.5 ± 0.3	Au ₅₂₃ (MDDS) ₇₂ (F6) ₄₉
NP-TMDA/F6-a	1 : 0.65	0.40	5.0 : 1	0.17	3.9 ± 0.9	Au ₂₄₀₆ (TMDA) ₂₅₆ (F6) ₅₁
NP-TMDA/F6-b	1 : 0.77	0.43	1.1 : 1	0.48	4.2 ± 0.7	Au ₂₄₀₆ (TMDA) ₁₃₁ (F6) ₁₁₉
NP-TMDA/F6-c	1 : 1.30	0.57	1.3 : 1	0.43	4.0 ± 0.9	Au ₂₄₀₆ (TMDA) ₁₆₀ (F6) ₁₂₄

^a H stands for the hydrogenated ligand. ^b determined on decomposed NPs by ¹H NMR spectra analysis. ^c Measured by TEM. ^d The average NPs composition was calculated considering TEM and TGA data.

In contrast to **NP-MUS/F8** and **NP-MDDS/F8**, nanoparticles **NP-MDDS/F6-a** were nicely soluble in water. In order to explore these types of NPs in more detail, different values of the **HMDDS/HF6** ratios were tested. Nanoparticles **NP-MDDS/F6-b** with a core diameter of 3.2 ± 0.7 nm and a **MDDS:F6** final molar ratio of 2.5:1 could be obtained by using an initial **MDDS:F6** ratio of 1.3:1; hence, also in this case the introduction of the **F6** thiolate in the monolayer of nanoparticles **NP-MDDS/F6-b** is disfavored. The nanoparticles **NP-MDDS/F6-c** with an average gold core diameter of 3.4 ± 0.7 nm and a mixed monolayer with a **MDDS:F6** molar ratio of 1.5:1 were obtained by using an initial **HMDDS:HF6** ratio of 1:0.9. With increasing amounts of F-ligand in the blend used for the synthesis up to a **HMDDS:HF6** ratio of 1:2, the NPs were only soluble in fluorinated solvents such as trifluorotoluene.

The preparation of the H-/F-mixed monolayer nanoparticles **NP-MDA/F6-a**, **NP-MDA/F6-b** and **NP-MDA/F6-c**, featuring carboxylic groups on the surface was achieved by using blends of the ligands **HMDA** and **HF6** of different composition while maintaining constant the gold to total thiol molar ratio. The nanoparticles were obtained by direct synthesis using ethanol as solvent and a dropwise addition of the reducing agent over 15 minutes. The relevant synthetic and characterization data are reported in Table 1.

Also with **HMDA** as hydrophilic ligand the molar fraction of the F-ligand in the self-assembled monolayer on the gold surface was lower than that used for the synthesis. All of these systems display good solubility in alcohols but are sparingly soluble in water. The average size of the gold core for the nanoparticles **NP-MDA/F6** is similar to those of NPs obtained by using the **MDDS/F6** blends, Table 1.

The preparation of H-/F-mixed monolayer NPs featuring a cationic surface was accomplished by using positively charged **HTMDA** in combination with **HF6**. As in the preceding examples, the preparation of the NPs was carried out by direct synthesis using a gold to thiols ratio of 3:2 while the **HTMDA/HF6** ratio used was set to 1:0.65 for **NP-TMDA/F6-a**; 1:0.77 for **NP-TMDA/F6-b** and 1:1.3 for **NP-TMDA/F6-c** and their characterization data are reported in Table 1. Also in this case the introduction of the **HF6** ligand in the monolayer of the NPs was found to be disfavored nicely matching the trend observed for the negatively charged and charge neutral nanoparticles **NP-MDDS/F6** and **NP-MDA/F6**, respectively. However, the size of the NPs core is slightly larger; see Table 1, than that obtained by using blends of thiols **HMDDS/HF6** and **HMDA/F6**, the standard deviation of the core size is also larger. All nanoparticles **NP-TMDA/F6** are soluble in methanol and ethanol and slightly soluble in water or basic buffers.

The introduction of polar end groups in the H-thiolates of nanoparticles **NP-MDDS/F6**, **NP-MDA/F6** and **NP-TMDA/F6** allows for the first time a solubility in water which was not observed for mixed ligand coated NPs featuring non-functionalized fluorinated thiolates.^{15,38}

A synoptic view of the solubility properties of **NP-MDDS/F6-b**, **NP-MDA/F6-c** and **NP-TMDA/F6-c** is presented in Figure 2A. The relation between the composition of the H- and F-ligands used in the NPs synthesis and the composition of the resulting mixed monolayer can be conveniently analyzed by plotting the final molar fraction of the F-component in the monolayer against the molar fraction of the fluorinated ligand in the reaction mixture, Figure 2B. By using thiol **HF8**, the final monolayer composition closely matches the initial composition of the reaction mixture; while for NPs preparations where thiol **HF6** was employed, the fraction of fluorinated thiolate was lower than its initial value. This is likely due to the combination of the lower number of fluorophilic interactions established between **F6** chains and their shorter length respect to **F8** chains. A similar effect was observed in the preparation of several mixed monolayer NPs protected by blends of unfunctionalized hydrogenated thiolates and *1H,1H,2H,2H*-perfluoro-alkanethiolates.³⁸

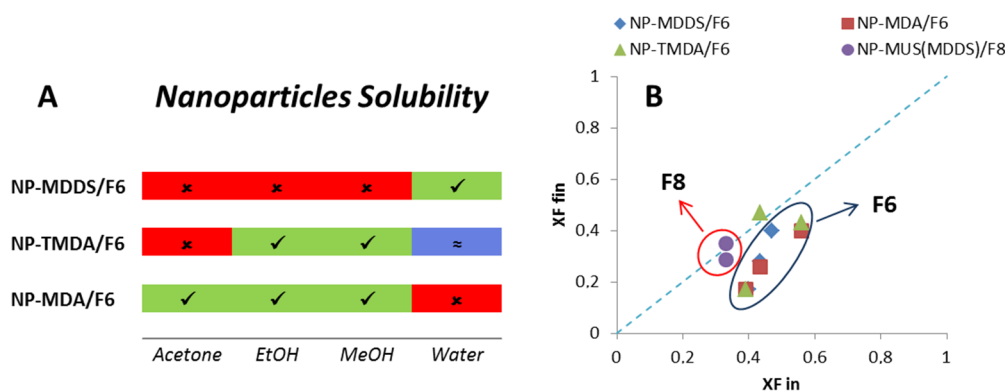


Figure 2. Panel A: synoptic view of the solubility properties of the H-/F-mixed monolayer NPs. Color code: red insoluble; green good solubility; indigo low solubility. Panel B: relationship between the initial composition of the reaction mixture and the final composition of the monolayer of the NPs expressed as the molar fraction of the F-ligand.

Given the appreciable solubility of the nanoparticles **NP-MDDS/F6** and **NP-TMDA/F6** in aqueous media; these systems were used for cell uptake and cytotoxicity studies. For comparison purposes, homoligand – charge neutral – AuNPs **NP-C8TEG** and **NP-F8PEG** were prepared by using the ligands **HC8TEG** and **HF8PEG**, Figure 1B, according to procedures already reported by our group.^{40,41}

Tagging of gold nanoparticles with fluorescent labels. Nanoparticles **NP-MDDS/F6-b**; **NP-TMDA/F6-c**; **NP-C8TEG** and **NP-F8PEG**, were labeled with a fluorescent ligand in order to monitor the internalization process by confocal fluorescence microscopy and cytofluorimetric analyses. For labeling we used the Bodipy functionalized thiol **HBodipy**,¹³ Figure 1C, obtaining the nanoparticles **NP-C8TEG/Bodipy**, **NP-F8PEG/Bodipy**, **NP-MDDS/F6/Bodipy** and **NP-TMDA/F6/Bodipy**, Table 2. The fluorescent units were introduced in the monolayer of the NPs by place exchange; the NPs were dissolved in water or methanol, and the appropriate amount of the **HBodipy** was added as a 1.95 mM solution in a water/DMF 4:1 mixture. The place exchange reaction was performed for 3 days at 28 °C. The degree of substitution was established by decomposing the NPs and assessing the amount of dye in solution by means of UV-Vis spectroscopy and the resulting compositions are reported in Table 2.

Table 2. Characterization data of the Bodipy labeled nanoparticles.

Sample	BODIPY units per NP	Nanoparticle Composition
NP-F8PEG/Bodipy	6	Au ₉₇₆ (F8PEG) ₁₁₄ (BODIPY) ₆
NP-C8TEG/Bodipy	2	Au ₇₆₀ (C8TEG) ₁₆₈ (BODIPY) ₂
NP-MDDS/F6/Bodipy	6	Au ₁₂₈₉ (MDDS/F6) ₂₀₄ (BODIPY) ₆
NP-TMDA/F6/Bodipy	5	Au ₂₄₀₆ (TMDA/F6) ₂₇₉ (BODIPY) ₅

For all NPs the amount of fluorescent dye introduced in the ligand shell was kept lower than 10 units per nanoparticle to avoid increasing the hydrophobicity of the NPs' surface and, in general, modifying the features of the monolayer.

Nanoparticles interaction with HeLa cells. The uptake of charged H-/F- mixed monolayer coated nanoparticles **NP-MDDS/F6/Bodipy** and **NP-TMDA/F6/Bodipy** by HeLa cells was assessed by FACS analysis and fluorescence confocal microscopy imaging and compared to the uptake of the charge neutral homoligand nanoparticles **NP-C8TEG/Bodipy** and **NP-F8PEG/Bodipy**. Prior to study the interaction with HeLa cells, the presence of free dye or free dye-labeled thiol **HBodipy** in the NPs preparations was tested by the red blood cells (RBCs) assay⁴² and no free dye could be detected, see Figure S22 and Figure S23. For the internalization studies the HeLa cells were plated at 3×10^5 cells/mL in complete medium (with serum) and allowed to grow overnight. The cells were incubated with Bodipy labeled NPs at the concentrations of 0.05, 0.1 and 0.2 mg/mL for 3.5 hours at 37°C and imaged live by confocal laser scanning microscopy (CLSM). Cellular internalization of the Bodipy labeled NPs is shown by red fluorescence, the nucleus (in blue) was stained with Hoechst 33342. For all samples, cellular uptake is clear from confocal images with intense fluorescence signal in the cytosol and absence in the nucleus.

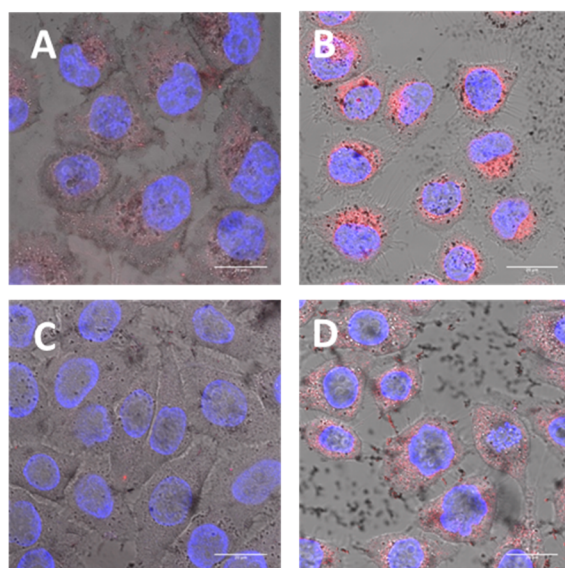


Figure 3. Confocal fluorescence micrographs merged with light microscopy images of HeLa cells incubated for 3.5 hours at 37 °C at a concentration of 0.1 mg/mL with **NP-MDDS/F6/Bodipy**, (panel A), scale bar: 20 μ m. Panel B: **NP-TMDA/F6/Bodipy**, scale bar: 20 μ m. Confocal fluorescence micrographs merged with light microscopy images of HeLa cells incubated for 3.5 hours at 4 °C at a concentration of 0.1 mg/mL with **NP-MDDS/F6/Bodipy** (panel C), scale bar: 20 μ m. Panel D: **NP-TMDA/F6/Bodipy**, scale bar: 20 μ m. The nucleus in all experiments was stained by Hoechst 33342 (blue).

At 37°C, both the negatively and positively charged nanoparticles **NP-MDDS/F6/Bodipy** and **NP-TMDA/F6/Bodipy** were internalized, Figure 3A and Figure 3B, with a higher uptake in case of the positively charged NPs. At 4°C, a temperature at which the endocytic and pinocytic uptake pathways are inhibited, no fluorescence could be observed in the cytoplasm of HeLa cells treated with **NP-MDDS/F6/Bodipy**, Figure 3C, while in the case of **NP-TMDA/F6/Bodipy**, the cell cytoplasm displayed a significant red fluorescence, Figure 3D. This is clear indication that that the negatively charged particles are mainly internalized by an active energy dependent pathway while the positive particles are able to enter through the membrane into the cytosol of the cell.

A similar effect has been reported for other cationic NPs^{43,44} and *in silico* analyses of the process^{45,46} explain it by NPs entry through nanosized holes in the plasma membrane usually connected to significant cytotoxicity.

Accordingly, the cytotoxicity of the tested nanoparticles was determined by FACS analyses, Figure 4. For this, HeLa cells were incubated with NPs for 3.5 hours at the concentrations of 0.05 mg/mL, 0.1 mg/mL and 0.2 mg/mL. Then the non-membrane permeable fluorescent DNA-binding propidium iodide (PI) was used to determine cell membrane integrity.

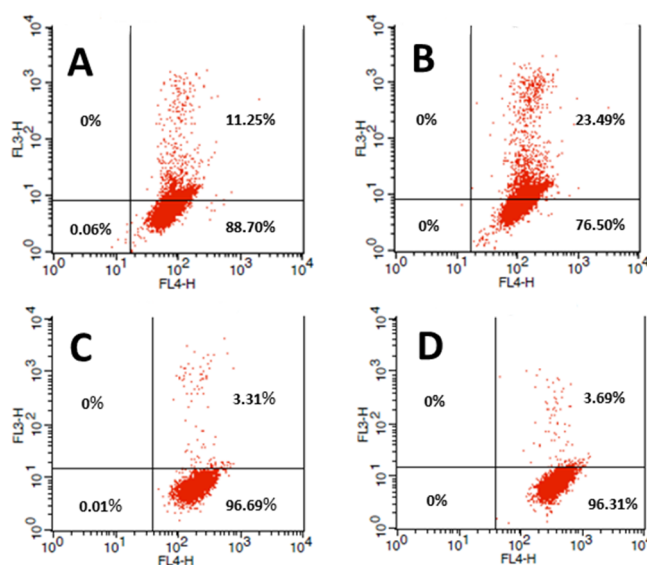


Figure 4. FACS analysis of HeLa cells incubated for 3.5 hours at 37 °C with **NP-MDDS/F6/Bodipy** at a concentration of 0.05 mg/mL (panel A) and of 0.1 mg/mL (panel B), or with **NP-TMDA/F6/Bodipy** at a concentration of 0.05 mg/mL (panel C) and of 0.1 mg/mL (panel D).

We observed that the negatively charged **NP-MDDS/F6/Bodipy** showed limited cytotoxicity to moderate toxicity in a concentration dependent manner with 38% of the cell population labeled with both NPs and PI indicating disruption of the cell membrane at a concentration of 0.2 mg/mL (Figure S24). In an assessment of NPs toxicity towards mammalian cells, Rotello and coworkers,⁴⁷ reported that anionic NPs, featuring for instance carboxylate groups on their surface, are less toxic than

cationic NPs, with the anionic displaying LC_{50} values about one order of magnitude higher than the cationic. Surprisingly, we found that the positively charged **NP-TMDA/F6/Bodipy** showed at maximum 7% of PI positive cells after exposure to the highest tested NPs concentration of 0.2 mg/mL (Figure S25). These percentages are comparable to those measured for untreated control cells. The limited toxicity of **NP-TMDA/F6/Bodipy** may imply that these cationic nanoparticles, at the concentrations tested, do not exert extensive damage to the plasma membrane upon internalization. For similar cationic hydrogenated nanoparticles Rotello and coworkers, reported a LC_{50} of about 1 μ M; in the case of **NP-TMDA/F6/Bodipy** the highest concentration tested for which we could not observe cytotoxic effects was 0.2 mg/mL, corresponding to 0.35 μ M, that is significantly lower than the LC_{50} value reported. It is thus intriguing that the anionic **NP-MDDS/F6/Bodipy**, instead, exert a significantly higher toxic effect than **NP-TMDA/F6/Bodipy** when tested at similar concentration levels. However, a recent thorough investigation of nanoparticles toxicities, by Stellacci and Pompa,³⁵ on six cell lines, including HeLa cells, displays that nanoparticles presenting sulfonate groups on their surface and whose monolayer featured stripe-like domains remains essentially non cytotoxic at the same concentration at which non-structured anionic nanoparticles exert a cytotoxic effect. It is not unlikely that in the case of **NP-MDDS/F6/Bodipy** the toxic effects observed are due to the organization of the monolayer. This hypothesis is also corroborated by the absence of internalization at 4 °C for nanoparticles **NP-MDDS/F6/Bodipy** which might be expected if these nanoparticles present a stripe-like organization of the monolayer in analogy to similar mixed monolayer nanoparticles.²⁴

The charge neutral nanoparticles **NP-C8TEG/Bodipy** and **NP-F8PEG/Bodipy** were also efficiently internalized at 37 °C, as evidenced by the strong intensity of the red fluorescence in Figure 5A and Figure 6A respectively. By performing the same experiments at 4 °C, cellular uptake of **NP-C8TEG/Bodipy** or **NP-F8PEG/Bodipy**, Figure 6B and Figure 6B respectively, was inhibited.

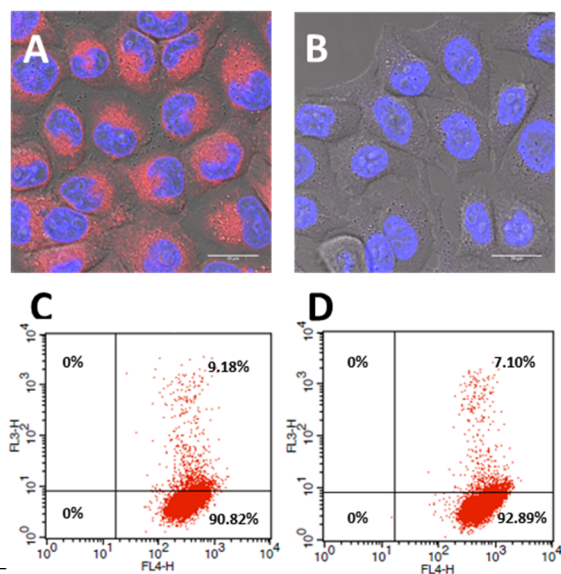


Figure 5. Merged light microscopy and confocal fluorescence images of HeLa cells incubated with NPs at a concentration of 0.1 mg/mL for 3.5 hours with **NP-C8TEG/Bodipy** at 37 °C (A) **NP-C8TEG/Bodipy** or at 4 °C (B), scale bars: 20 μ m. FACS analysis of HeLa cells incubated for 3.5 hours with **NP-C8TEG/Bodipy** at a concentration of 0.05 mg/mL (C) or 0.1 mg/mL (D).

Cytofluorimetric analyses for **NP-C8TEG/Bodipy** showed no significant cytotoxicity; for all concentrations tested more than 90 % of the cells were viable after incubation with 0.05 and 0.1 mg/mL of the NPs for 3.5 hours, Figure 5C and Figure 5D respectively.

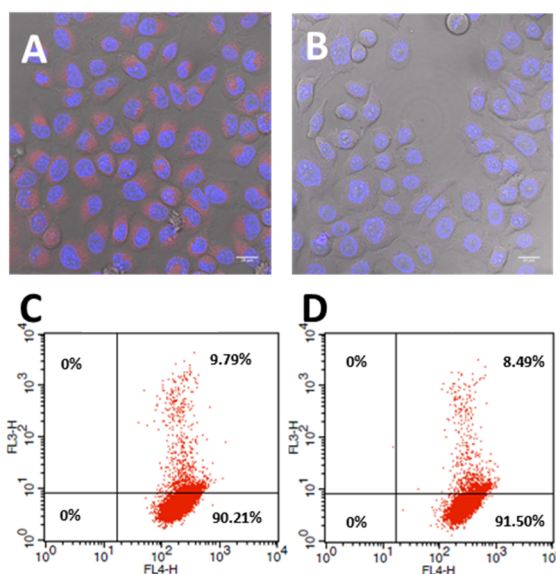


Figure 6. Merged light microscopy and confocal fluorescence images of HeLa cells incubated with NPs at a concentration of 0.1 mg/mL for 3.5 hours with **NP-F8PEG/Bodipy** at 37 °C (A) or at 4 °C (B), scale bars: 20 μ m. FACS analysis of HeLa cells incubated for 3.5 hours with **NP-F8PEG/Bodipy** at a concentration of 0.05 mg/mL (C) or 0.1 mg/mL (D).

At the higher concentration of 0.2 mg/mL, (Figure S26), the percentage of dead cells remains fairly constant and close to that measured in control experiments with untreated cells.

Nanoparticles **NP-F8PEG/Bodipy**, gave similar results up to the concentration of 0.05 and 0.1 mg/mL, Figure 6C and Figure 6D respectively, while at the higher concentration tested, some cytotoxicity could be observed. Indeed, after exposure to 0.2 mg/mL of **NP-F8PEG/Bodipy** the percentage of PI stained cells containing NPs was 16% (Figure S27). These data are in line with the toxicity of other homoligand PEG decorated fluorinated NPs.¹³

Conclusions

In this proof-of-principle study the preparation of a series of mixed H-/F-mixed monolayer AuNPs featuring cationic and anionic surfaces was achieved by direct synthesis using blends of simple hydrogenated thiols with charged end groups and commercially available 1*H*,1*H*,2*H*,2*H*-perfluoro-alkanethiols. The exploration of the ligands structure highlights that the length of the fluorinated thiol or, most likely, the difference in length between the hydrogenated and fluorinated ligands is a critical parameter to be considered for obtaining NPs with acceptable solubility properties. The fluorinated thiol has to be short enough, compared to the hydrogenated ligand, to form fluorinated domains that are sufficiently small to be masked from the solvent. In the present study we explored this aspect and found that the thiol **HF8** is too long, producing NPs that are poorly soluble; on the contrary, the use of the two CF₂ units shorter **HF6**, gave NPs with improved solubility. By this approach we achieved a tremendous broadening of the solvents spectrum in which H-/F-mixed monolayer NPs can be studied, including acetone, alcohols and, most notably, water. At variance with previous examples, the systems presented here carry specific charged moieties paving the way to applications and studies thus far out of reach. The solubility in aqueous media of anionic **NP-MDDS/F6** and cationic **NP-TMDA/F6** nanoparticles, though not yet optimal, allowed performing some preliminary uptake and cytotoxicity studies towards HeLa cells. Both the charged nanoparticle systems were readily internalized but in uptake studies performed at 4°C only **NP-TMDA/F6** were found to enter the cells, suggesting that different internalization pathways are available to the different NPs. Nanoparticles **NP-TMDA/F6** displayed only a limited toxicity and were well tolerated by the cells up to a concentration of 0.2 mg/ml indicating that despite the cationic nature of this system, at this concentration there is little perturbation of the cell membrane. Instead nanoparticles **NP-MDDS/F6** displayed some cytotoxicity when tested at the same concentration. The charge neutral homoligand nanoparticles **NP-C8TEG** and **NP-F8PEG** were also tested for their cytotoxicity and while the former were found to be non-toxic at all the concentration tested, the latter displayed some cytotoxicity when used at a concentration of 0.2 mg/ml. Overall, the cationic nanoparticles **NP-TMDA/F6** display toxicity similar to that of the charge neutral NPs. Given the well-established tendency of fluorinated thiolates to self-sort on the surface of AuNPs

and the now available synthetic strategies to charged H-/F- mixed monolayer AuNPs we are confident that these systems, after further structural refinement, will significantly widen the span of NPs systems with anisotropic monolayers to probe the interactions of nanosized matter with the biological environment.

Experimental Procedures

Synthesis of NP-MDDS/F6-a. A 250 mL three neck round bottom flask was charged with 88.8 mg (2.29×10^{-4} mol, 1 equiv.) of $\text{HAuCl}_4 \cdot 3\text{H}_2\text{O}$ dissolved in 50 mL of deoxygenated ethanol and 1.52×10^{-4} mol (0.66 equiv.) of the thiols mixture (**HF6** : **HMDDS** = 0.65 : 1). Then a 0.11 M solution of NaBH_4 in deoxygenated ethanol (2.59×10^{-3} mol, 11.3 equiv.) was added dropwise over 15 minutes. The solution becomes brown-reddish and some precipitation of NPs was observed. The mixture was stirred for 3 hours at room temperature and afterwards, the reaction vessel was then kept at 4 °C overnight; the precipitated NPs were collected and the solvent was discarded. The NPs were washed with ethanol, methanol and acetone and dried under vacuum. To completely remove unbound ligands, particles were dialyzed against 1 liter of MilliQ water for a total time span of 72 hours; the system was recharged with fresh water every 8 hours. The NPs solution was collected and the solvent was removed under vacuum at a temperature lower than 45 °C obtaining the NPs as a red solid. The final ratio between **MDDS** : **F6** was 5 : 1. Solubility properties: Good solubility in water. Not soluble in ethanol, methanol and acetone. UV-Vis (water) λ_{max} (nm): Weak surface plasmon band at 508 nm. ^1H NMR (500 MHz, D_2O): $\delta = 0.9 - 1.60$ (br, CH_2), 1.77 (br, $\text{CH}_2\text{CH}_2\text{SH}$ and $\text{CH}_2\text{CH}_2\text{SO}_3\text{Na}$), 2.88 (br, $\text{CH}_2\text{SO}_3\text{Na}$). TEM: $X_m = 3.1$ nm; $\sigma = 0.8$ nm; $n = 134$. TG Analysis: 19.5 %. Average composition: $\text{Au}_{1150}(\text{MDDS})_{145}(\text{F6})_{29}$.

Synthesis of NP-MDDS/F6-b. A 250 mL round bottom flask was charged with 100 mg (2.54×10^{-4} mol, 1 equiv.) of $\text{HAuCl}_4 \cdot 3\text{H}_2\text{O}$ dissolved in 56 mL of deoxygenated ethanol and 1.69×10^{-4} mol (0.66 equiv.) of the thiols mixture (**HF6** : **HMDDS** = 0.77 : 1). Then a 0.11 M solution of NaBH_4 in deoxygenated ethanol (2.87×10^{-3} mol, 11.3 equiv.) was added dropwise over 17 minutes. The solution becomes brown-reddish and some precipitation of NPs was observed. The mixture was stirred for 3 hours at room temperature and afterwards the reaction vessel was kept at 4 °C overnight; the precipitated NPs were collected and the solvent was discarded. The NPs were washed with ethanol, methanol and acetone and dried under vacuum. The NPs were dialyzed against 1 liter of MilliQ water for 72 hours recharging the system with fresh water every 8 hours. The NPs solution was collected and the solvent was removed under reduced pressure working at temperature below 45 °C. The residue was washed several times with hot ethanol to remove unbound thiols. The

final ratio between **MDDS** : **F6** was 2.5 : 1. Solubility properties: Good solubility in water. Not soluble in ethanol, methanol and acetone. UV-Vis (water) λ_{\max} (nm): Weak surface plasmon band at 508 nm. ^1H NMR (500 MHz, D_2O): $\delta = 0.9 - 1.60$ (br, CH_2), 1.77 (br, $\text{CH}_2\text{CH}_2\text{SH}$ and $\text{CH}_2\text{CH}_2\text{SO}_3\text{Na}$), 2.88 (br, $\text{CH}_2\text{SO}_3\text{Na}$). TEM: $X_m = 3.2$ nm; $\sigma = 0.7$ nm; $n = 253$. TG Analysis: 21%. Average composition: $\text{Au}_{1289}(\text{MDDS})_{150}(\text{F6})_{60}$.

Synthesis of NP-MDDS/F6-c. A 250 mL round bottom flask was charged with 97.3 mg (2.47×10^{-4} mol, 1 equiv.) of $\text{HAuCl}_4 \cdot 3\text{H}_2\text{O}$ dissolved in 55 mL of deoxygenated ethanol and 1.65×10^{-4} mol (0.66 equiv.) of the thiols mixture (**HF6** : **HMDDS** = 1 : 1.1). Then a 0.11 M solution of NaBH_4 in deoxygenated ethanol (2.80×10^{-3} mol, 11.3 equiv.) was added dropwise over 12 minutes. The solution becomes brown-reddish observing some precipitation of NPs. The mixture was stirred for 3 hours at room temperature and afterwards the reaction vessel was then kept at 4 °C overnight; the precipitated NP were collected and the solvent was discarded. The NPs were washed with ethanol, methanol and acetone and dried under vacuum. The NPs were taken up with water and dialyzed against MilliQ water for 72 hours recharging the system with fresh water every 8 hours. The NPs solution was collected and the solvent was removed under reduced pressure working at a temperature lower than 45 °C. To completely remove unbound ligands NPs were washed several times with hot ethanol. The final ratio between **MDDS** : **F6** was 1.5 : 1. Solubility properties: Good solubility in water. Not soluble in ethanol, methanol and acetone. UV-Vis (water) λ_{\max} (nm): Weak surface plasmon band at 510 nm. ^1H NMR (500 MHz, D_2O): $\delta = 0.9 - 1.60$ (br, CH_2), 1.77 (br, $\text{CH}_2\text{CH}_2\text{SH}$ and $\text{CH}_2\text{CH}_2\text{SO}_3\text{Na}$), 2.88 (br, $\text{CH}_2\text{SO}_3\text{Na}$). TEM: $X_m = 3.4$ nm; $\sigma = 0.7$ nm; $n = 209$. TG Analysis: 16%. Average composition: $\text{Au}_{1415}(\text{MDDS})_{129}(\text{F6})_{87}$.

Synthesis of NP-MDA/F6-a. A 250 mL round bottom flask was charged with 80 mg (0.20×10^{-3} mol, 1 equiv.) of $\text{HAuCl}_4 \cdot 3\text{H}_2\text{O}$ dissolved in 44 mL of deoxygenated ethanol and 0.14×10^{-3} mol (0.66 equiv.) of the thiols mixture (**HF6**: **HMDA** = 0.65 : 1). Then a 0.11 M solution of NaBH_4 in deoxygenated ethanol (2.3×10^{-3} mol, 11.3 equiv.) was added dropwise over 15 minutes. The mixture was stirred for 3 hours and the reaction vessel was then kept at 4 °C overnight; the precipitated NPs were collected and the solvent was discarded. The precipitated NPs were washed with ethanol and acetone and dried under vacuum. The NPs were dialyzed against MilliQ water for 72 hours recharging the system with fresh water ca. every 8 hours. The NP solution was collected and the solvent was removed under vacuum working at temperature below 45 °C. The NPs were further purified by size exclusion chromatography on Sephadex LH-20 using methanol as eluent. The final ratio between **MDA**: **F6** was 5 : 1. Solubility properties: Good solubility in ethanol,

methanol and acetone. UV-Vis (water) λ_{\max} (nm): Weak surface plasmon band at 500 nm. ^1H NMR (500 MHz, D_2O): $\delta = 1.10 - 1.50$ (br, CH_2), 1.60 (br, $\text{CH}_2\text{CH}_2\text{SH}$ and $\text{CH}_2\text{CH}_2\text{COOH}$), 2.85 (br, CH_2COOH) ppm. TEM: $X_m = 3.01$ nm; $\sigma = 0.52$ nm; $n = 234$. TG Analysis: 20 %. Average composition: $\text{Au}_{976}(\text{MDA})_{136}(\text{F6})_{28}$.

Synthesis of NP-MDA/F6-b. A 250 mL round bottom flask was charged with 99.3 mg (0.25×10^{-3} mol, 1 equiv.) of $\text{HAuCl}_4 \cdot 3\text{H}_2\text{O}$ dissolved in 56 mL of deoxygenated ethanol and 0.17×10^{-3} mol (0.67 equiv.) of the thiols mixture (**HF6** : **HMDA** = 0.76 : 1). Then a 0.11 M solution of NaBH_4 in deoxygenated ethanol (2.83×10^{-3} mol, 11.3 equiv.) was added dropwise over 15 minutes. The mixture was stirred for 3 hours and the reaction vessel was then kept at 4 °C overnight; the precipitated NP were collected and the solvent was discarded. The precipitated NPs were washed with ethanol (3 x 20 mL), acetone (3 x 20 mL) and DCM (3 x 20 mL) and dried under vacuum obtaining 43.4 mg of NPs. The final ratio between **MDA** : **F6** was 2.9 : 1. Solubility properties: Low solubility in ethanol, and acetone, good solubility in methanol. UV-Vis (methanol) λ_{\max} (nm): Weak surface plasmon band at 523 nm. ^1H NMR (500 MHz, CD_3OD): $\delta = 1.10 - 1.50$ (br, CH_2), 1.60 (br, $\text{CH}_2\text{CH}_2\text{SH}$ and $\text{CH}_2\text{CH}_2\text{COOH}$), 2.19 (br, CH_2COOH) ppm. TEM: $X_m = 2.45$ nm; $\sigma = 0.56$ nm; $n = 488$. TG Analysis: 33 %. Average composition: $\text{Au}_{523}(\text{MDA})_{90}(\text{F6})_{30}$.

Synthesis of NP-MDA/F6-c. A three neck round bottom flask was charged with 81.8 mg (2.08×10^{-4} mol, 1 equiv.) of $\text{HAuCl}_4 \cdot 3\text{H}_2\text{O}$ dissolved in 45 mL of deoxygenated ethanol and 1.38×10^{-4} mol (0.66 equiv.) of the thiols mixture (**HF6** : **HMDA** = 1.3 : 1). Then a 0.11 M solution of NaBH_4 in deoxygenated ethanol (2.35×10^{-3} mol, 11.3 equiv.) was added dropwise over 11 minutes. The mixture was stirred at room temperature for 3 hours and then the NPs were precipitated by addition of hexane. The precipitate was repeatedly washed with hexane and the crude material was further purified by gel permeation chromatography on Sephadex LH-20 using methanol as eluent. The purified NPs were obtained as a brown-red solid. The final ratio between **MDA** : **F6** was 1.5 : 1. Solubility properties: Good solubility in ethanol, methanol and acetone. UV-Vis (water) λ_{\max} (nm): Weak surface plasmon band at 508 nm. ^1H NMR (500 MHz, CD_3OD): $\delta = 0.9 - 1.50$ (br, CH_2), 1.60 (br, $\text{CH}_2\text{CH}_2\text{SH}$ and $\text{CH}_2\text{CH}_2\text{COOH}$), 2.25 (br, CH_2COOH). TEM: $X_m = 2.5$ nm; $\sigma = 0.3$ nm; $n = 204$. Average composition: $\text{Au}_{523}(\text{MDA})_{72}(\text{F6})_{49}$.

Synthesis of NP-TMDA/F6-a. A 250 mL three neck round bottom flask was charged with 80 mg (2.03×10^{-4} mol, 1 equiv.) of $\text{HAuCl}_4 \cdot 3\text{H}_2\text{O}$ dissolved in 44 mL of deoxygenated ethanol and 1.35×10^{-4} mol (0.66 equiv.) of the thiols mixture (**HF6** : **HTMDA** = 0.65 : 1). Then a 0.11 M solution of

NaBH₄ in deoxygenated ethanol (2.3 x 10⁻³ mol, 11.3 equiv.) was added dropwise over 15 minutes. The solution becomes brown observing some precipitation of the NPs. The mixture was stirred for 3 hours and the reaction vessel was then kept at 4 °C overnight; the precipitated NPs were collected and the solvent was discarded. The crude material was repeatedly washed with DCM to remove unbound ligands. The final ratio between **TMDA** : **F6** is 5 : 1. Solubility properties: soluble in methanol, ethanol, low solubility in water. UV-Vis (water) λ_{max} (nm): surface plasmon band at 525 nm. ¹H NMR (500 MHz, CD₃OD): δ = 3.33 (br, CH₂N(CH₃)₃), 3.17 (br, N(CH₃)₃), 1.78 (br, CH₂CH₂N(CH₃)₃), 1.60-0.9 (br, CH₂). TEM: X_m = 3.9 nm; σ = 0.9 nm; n = 583. TG Analysis: 19%. Average composition: Au₂₄₀₆(TMDA)₂₅₆(F6)₅₁.

Synthesis of NP-TMDA/F6-b. A 250 mL three neck round bottom flask was charged with 101 mg (0.25 x 10⁻³ mol, 1 equiv.) of HAuCl₄·3H₂O dissolved in 56 mL of deoxygenated ethanol and 0.169 x 10⁻³ mol (0.68 equiv.) of the thiols mixture (**HF6** : **HTMDA** = 0.77 : 1). Then a 0.11 M solution of NaBH₄ in deoxygenated ethanol (2.88 x 10⁻³ mol, 11.3 equiv.) was added dropwise over 20 minutes. The solution becomes brown observing some precipitation of the NPs; the mixture was stirred for 3. The precipitated NPs were collected and the solvent discarded. The crude material was washed with acetone (3 x 20 mL), DCM (3 x 20 mL) and acetone (6 x 20 mL), the crude material was dissolved in few milliliters of methanol and the NPs were precipitated by adding hexane. The precipitate was washed with DCM (2 x 20 mL), acetone (2 x 20 mL) and DCM (2 x 5 mL) and dried obtaining 53.5 mg of clean NPs as a reddish solid. The final ratio between **TMDA** : **F6** was 1.1 : 1. Solubility properties: soluble in methanol, ethanol, low solubility in water. UV-Vis (water) λ_{max} (nm): surface plasmon band at 521 nm. ¹H NMR (500 MHz, CD₃OD): δ = 3.33 (br, CH₂N(CH₃)₃), 3.17 (br, N(CH₃)₃), 1.78 (br, CH₂CH₂N(CH₃)₃), 1.60-0.9 (br, CH₂). TEM: X_m = 4.16 nm; σ = 0.7 nm; n = 339. TG Analysis: 15%. Average composition: Au₂₄₀₆(TMDA)₁₃₁(F6)₁₁₉.

Synthesis of NP-TMDA/F6-c. A 250 mL three neck round bottom flask was charged with 98 mg (0.249 x 10⁻³ mol, 1 equiv.) of HAuCl₄·3H₂O dissolved in 54 mL of deoxygenated ethanol and 0.166 x 10⁻³ mol (0.66 equiv.) of the thiols mixture (**HF6** : **HTMDA** = 1.3 : 1). Then a 0.11 M solution of NaBH₄ in deoxygenated ethanol (2.82 x 10⁻³ mol, 11.3 equiv.) was added dropwise over 15 minutes. The solution becomes brown observing some precipitation of the NPs; the mixture was stirred for 3 hours and afterwards the reaction vessel was placed at 4 °C overnight. The precipitated NPs were collected and the solvent discarded. The crude material was washed with DCM obtaining 46 mg of clean NPs as a reddish solid. The final ratio between **TMDA** : **F6** was 1.3 : 1. Solubility properties: soluble in methanol, ethanol, low solubility in water. UV-Vis (water) λ_{max} (nm): surface

plasmon band at 525 nm. ^1H NMR (500 MHz, CD_3OD): $\delta = 3.33$ (br, $\text{CH}_2\text{N}(\text{CH}_3)_3$), 3.17 (br, $\text{N}(\text{CH}_3)_3$), 1.78 (br, $\text{CH}_2\text{CH}_2\text{N}(\text{CH}_3)_3$), 1.60-0.9 (br, CH_2). TEM: $X_m = 4.0$ nm; $\sigma = 0.9$ nm; $n = 362$. TG Analysis: 16%. Average composition: $\text{Au}_{2406}(\text{TMDA})_{160}(\text{F6})_{124}$.

Preparation of NP-MDDS/F6/Bodipy. In a 25 mL round bottom flask 11.4 mg of **NP-MDDS/F6-b** were dissolved by using 5 mL of deoxygenated mQ water under an argon atmosphere and 150 μL of a 1.94 mM solution of **HBodipy** in DMF/ H_2O 4/1 were added; the mixture was kept under stirring at 25 $^\circ\text{C}$ for 4 days. To completely remove unbound ligands, particles were dissolved in MilliQ water and dialyzed against milliQ water for a total time of 72 hours. The system was recharged with fresh water every 8 hours. The NPs solution was collected from the dialysis tube and used as such.

Preparation of NP-TMDA/F6/Bodipy. In a 25 mL round bottom flask 10 mg of **NP-TMDA/F6-c** were dissolved by using 5 mL of deoxygenated mQ water under an argon atmosphere and 150 μL of a 1.94 mM solution of **HBodipy** in DMF/ H_2O 4/1 were added; the mixture was kept under stirring at 25 $^\circ\text{C}$ for 4 days. The NPs were purified by dialysis against 1 liter of milliQ for a total time of 72 hours recharging the system with fresh water every 8 hours. The NPs solution was used as such.

Preparation of NPs-C8TEG/Bodipy. In a 25 mL round bottom flask 10 mg of **NP-C8TEG** were dissolved using 5 mL of deoxygenated methanol under an argon atmosphere and 150 μL of a 1.94 mM solution of **HBodipy** in DMF/ H_2O 4/1 were added; the mixture was kept under stirring at 25 $^\circ\text{C}$ for 4 days. The solvent was removed under reduced pressure at a temperature below 45 $^\circ\text{C}$. To completely remove unbound ligands, the NPs were purified by size exclusion chromatography by using Sephadex LH-20 and methanol as eluent.

Preparation of NP-F8PEG/Bodipy. In a 25 mL round bottom flask 10 mg of **NPs-F8PEG** were dissolved using 5 mL of deoxygenated methanol under an argon atmosphere and 150 μL of a 1.94 mM solution of **HBodipy** in DMF/ H_2O 4/1 were added; the mixture was kept under stirring at 25 $^\circ\text{C}$ for 4 days. The solvent was removed under reduced pressure at a temperature below 45 $^\circ\text{C}$. The NPs were purified by size exclusion chromatography by using Sephadex LH-20 and methanol as eluent.

Cell culture and fluorescence imaging. Human cervical carcinoma cells (HeLa) were grown in a standard culture media at 37 °C and in 95% air, 5% CO₂ atmosphere. Cells were seeded in a μ -Slide 8-well ibidi plate (Martinsried, Germany) at a density of 5×10^4 cells per well (1.0 cm²) and were allowed to adhere overnight. Before cell incubation with nanoparticles, the medium containing fetal bovine serum was replaced with serum-free medium to avoid unspecific binding of the NPs to serum proteins. Cells were then incubated with Bodipy labeled NP for 3.5 h at 37 °C. After incubation the cells were washed 3 times with PBS. Nuclei were counterstained with Hoechst 33342 (Invitrogen, Oregon, USA), according to the manufacturer's instructions. Cellular internalization of the fluorescently labeled NP was visualized with an inverted confocal laser scanning microscope (CLSM, Carl Zeiss LSM 510) equipped with a 63 \times /1.3 oil DIC objective, using excitation lines at 405 (Hoechst 33342) and 633 nm (Bodipy (650/665 nm)). ImageJ software was used for image analysis.

Cell Viability – FACS analysis. HeLa cell incubation with Bodipy labeled NPs in a concentration range of 0.05-0.2 mg/mL was performed as described above. After incubation, 5×10^5 cell were collected by trypsination and washed with PBS containing 1% BSA. The staining of nonviable cells was performed with Propidium Iodide (50 μ g/mL in PBS) for 5 minutes at room temperature. The samples were analyzed immediately on a flow cytometer (FACS Canto II, BD Biosciences) with excitation at 488 nm for PI and an excitation at 633 nm for Bodipy.

Associated Content

Supporting Information

Synthetic and characterization details of the ligands **MDDS**, **MDA**, **TMDA**, **NP-MUS/F8**, **NP-MDDS/F8**, **NP-C8TEG**, **NP-F8PEG**. Characterization data for the nanoparticles **NP-MDDS/F6**, **NP-MDA/F6** and **NP-TMDA/F6**. Results of the red blood assay for the nanoparticle systems **NP-MDDS/F6/Bodipy**, **NP-TMDA/F6/Bodipy**, **NP-C8TEG/Bodipy**, and **NP-F8PEG/Bodipy**. FACS analysis of HeLa cells incubated with 0.2 ml/mL of the nanoparticle systems. The Supporting Information is available free of charge on the ACS Publications website at DOI:

Author Information

Corresponding Authors

* E-mail: ppengo@units.it

* E-mail: lpassquato@units.it.

Acknowledgments

This work was financially supported by the Italian Ministry of Health, project GR-2009-1579849 and the University of Trieste (FRA Projects 2014, 2015).

References

1. Nishio, T., Niikura, K., Matsuo, Y., Ijro, K. (2010) Self-Lubricating Nanoparticles: Self-Organization into 3D-Superlattices During a fast Drying Process. *Chem. Commun.* 46, 8977-8979.
2. Niikura, K., Iyo, N., Higuchi, T., Nishio, T., Jinnai, H., Fujitani, N., Ijro, K. (2012) Gold Nanoparticles Coated with Semi-Fluorinated Oligo(ethylene glycol) Produce Sub-100 nm Nanoparticle Vesicles without Templates. *J. Am. Chem. Soc.* 134, 7632–7635.
3. Niikura, K., Iyo, N., Matsuo, Y., Mitomo, H., Ijro, K. (2013) Sub-100 nm Gold Nanoparticle Vesicles as a Drug Delivery Carrier enabling Rapid Drug Release upon Light Irradiation. *ACS Appl. Mater. Interfaces* 5, 3900–3907.
4. Ding, Y., Jiang, Z., Saha, K., Kim, C.-S., Kim, S.-T., Landis, R. F.; Rotello, V. M. (2014) Gold Nanoparticles for Nucleic Acid Delivery. *Mol. Ther.* 22, 1075–1083.
5. Ghosh, P., Han, G., De, M., Kim, C. K., Rotello, V. M. (2008) Gold Nanoparticles in Delivery Applications. *Adv. Drug Deliv. Rev.* 60, 1307–1315.
6. Ellipilli, S., Murthy, R. V., Ganesh, K. N. (2016) Perfluoroalkylchain Conjugation as a new Tactic for Enhancing Cell Permeability of Peptide Nucleic Acids (PNAs) *via* Reducing the Nanoparticle Size. *Chem. Commun.* 52, 521–524.
7. Rocha, S., Thünemann, A. F., Carmo Pereira, M., Coelho, M. A. N., Möhwald, H., Brezesinski, G. (2005) The Conformation of B18 Peptide in the Presence of Fluorinated and Alkylated Nanoparticles. *ChemBioChem* 6, 280–283.
8. Rocha, S., Thünemann, A. F., do Carmo Pereira, M., Coelho, M., Möhwald, H., Brezesinski, G. (2008) Influence of Fluorinated and Hydrogenated Nanoparticles on the Structure and Fibrillogenesis of Amyloid Beta-Peptide. *Biophys. Chem.* 137, 35–42.
9. Bocalon, M., Bidoggia, S., Romano, F., Gualandi, F., Franchi, P., Lucarini, M., Pengo, P., Pasquato, L. (2015) Gold Nanoparticles as Drug Carriers: a Contribution to the Quest for Basic Principles for Monolayer Design. *J. Mater. Chem. B* 3, 432–439.
10. Ma, S., Zhou, J., Wali, A. R. M., He, Y., Xu, X., Tang, J. Z., Gu, Z. (2015) Self-assembly of pH-Sensitive Fluorinated Peptide Dendron Functionalized Dextran Nanoparticles for On-Demand Intracellular Drug Delivery. *J. Mater. Sci.: Mater. Med.* 26, 219.

11. Porsch, C., Zhang, Y., Östlund, Å., Damberg, P., Ducani, C., Malmström, E., Nyström, A. M. (2013) In Vitro Evaluation of Non-Protein Adsorbing Breast Cancer Theranostics Based on ^{19}F -Polymer Containing Nanoparticles. *Part. Part. Syst. Charact.* 30, 381–390.
12. Janjic, J. M., Srinivas, M., Kadayakkara, D. K. K., Ahrens, E. T. (2008) Self-delivering Nanoemulsions for Dual Fluorine-19 MRI and Fluorescence Detection. *J. Am. Chem. Soc.* 130, 2832–2841.
13. Boccalon, M., Franchi, P., Lucarini, M., Delgado, J. J., Sousa, F., Stellacci, F., Zucca, I., Scotti, A., Spreafico, R., Pengo, P., *et al.* (2013) Gold Nanoparticles Protected by Fluorinated Ligands for ^{19}F MRI. *Chem. Commun.* 49, 8794–8796.
14. Posocco, P., Gentilini, C., Bidoggia, S., Pace, A., Franchi, P., Lucarini, M., Fermeglia, M., Pricl, S., Pasquato, L. (2012) Self-Organization of Mixtures of Fluorocarbon and Hydrocarbon Amphiphilic Thiolates on the Surface of Gold Nanoparticles. *ACS Nano* 6, 7243–7253.
15. Şologan, M., Marson, D., Polizzi, S., Pengo, P., Boccardo, S., Pricl, S., Posocco, P., Pasquato, L. (2016) Patchy and Janus Nanoparticles by Self-Organization of Mixtures of Fluorinated and Hydrogenated Alkanethiolates on the Surface of a Gold Core. *ACS Nano*, 10, 9316–9325.
16. Gentilini, C., Franchi, P., Mileo, E., Polizzi, S., Lucarini, M., Pasquato, L. (2009) Formation of Patches on 3D SAMs Driven by Thiols with Immiscible Chains Observed by ESR Spectroscopy. *Angew. Chem. Int. Ed.* 48, 3060–3064.
17. Elbert, R., Folda, T., Ringsdorf, H. (1984) Saturated and Polymerizable Amphiphiles with Fluorocarbon Chains. Investigation in Monolayers and Liposomes. *J. Am. Chem. Soc.* 106, 7687–7692.
18. Yoder, N. C., Kalsani, V., Schuy, S., Vogel, R., Janshoff, A., Kumar, K. (2007) Nanoscale Patterning in Mixed Fluorocarbon-Hydrocarbon Phospholipid Bilayers. *J. Am. Chem. Soc.* 129, 9037–9043.
19. Overnay, R. M., Meyer, E., Frommer, J., Brodbeck, D., Luthi, R., Howland, L., Guntherodt, H.-J., Fujihara, M., Takano, H., Gotoh, Y. (1992) Friction measurements on phase-separated thin films with a modified atomic force microscope. *Nature*, 359, 133–135.
20. Schönherr, H., Ringsdorf, H. (1996) Self-Assembled Monolayers of Symmetrical and Mixed Alkyl Fluoroalkyl Disulfides on Gold. 1. Synthesis of Disulfides and Investigation of Monolayer Properties. *Langmuir* 12, 3891–3897.
21. M. Jaschke, M., Schönherr, H., Wolf, H. Butt, H.-J., Bamberg, E., Besocke, M. K., Ringsdorf, H. (1996) Structure of Alkyl and Perfluoroalkyl Disulfide and Azobenzenethiol Monolayers on Gold(111) Revealed by Atomic Force Microscopy. *J. Phys. Chem.* 100, 2290–2301.

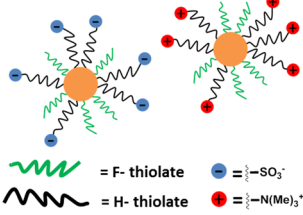
22. Schönherr, H., Ringsdorf, H., Jaschke, M., Butt, H.-J., Bamberg, E., Allinson, H., Evans, S. D. (1996) Self-Assembled Monolayers of Symmetrical and Mixed Alkyl Fluoroalkyl Disulfides on Gold. 2. Investigation of Thermal Stability and Phase Separation. *Langmuir* 12, 3898-3904.
23. Tsao, M.-W., Rabolt, J. F., Schönherr, H., Castner, D. G. (2000) Semifluorinated/Hydrogenated Alkylthiol Thin Films: A Comparison between Disulfides and Thiol Binary Mixtures. *Langmuir* 16, 1734-1743.
24. Jackson, A. M., Myerson, J. W., Stellacci, F. (2004) Spontaneous Assembly of Subnanometre-Ordered Domains in the Ligand Shell of Monolayer-Protected Nanoparticles *Nature Mater.* 3, 330–336.
25. Jackson, A. M., Hu, Y., Silva, P. J., Stellacci, F. (2006) From Homoligand- to Mixed-Ligand-Monolayer-Protected Metal Nanoparticles: A Scanning Tunneling Microscopy Investigation *J. Am. Chem. Soc.*, 128, 11135–11149.
26. Sing, C., Ghorai, P. K., Horsch, M. A., Jackson, A. M., Larson, R. G., Stellacci, F., Glotzer, S. C. (2007) Entropy-Mediated Patterning of Surfactant-Coated Nanoparticles and Surfaces *Phys. Rev. Lett.* 99, 226106.
27. Ghorai, P. K., Glotzer, S. C. (2010) Atomistic Simulation Study of Striped Phase Separation in Mixed-Ligand Self-Assembled Monolayer Coated Nanoparticles *J. Phys. Chem. C* 114, 19182–19187.
28. Pillai, P. P., Huda, S., Kowalczyk, B., A. Grzybowski, B. A. (2013) Controlled pH Stability and Adjustable Cellular Uptake of Mixed-Charge Nanoparticles. *J. Am. Chem. Soc.* 135, 6392–6395.
29. Hühn, D., Kantner, K., Geidel, C., Brandholt, S., De Cock, I., Soenen, S. J. H., Rivera-Gil, P., Montenegro, J.-M., Braeckmans, K., Müllen, K., *et al.* (2013) Polymer-Coated Nanoparticles Interacting with Proteins and Cells: Focusing on the Sign of the Net Charge. *ACS Nano* 7, 3253–3263.
30. Mout, R., Moyano, D. F., Rana, S., Rotello, V. M. (2012) Surface Functionalization of Nanoparticles for Nanomedicine. *Chem. Soc. Rev.* 41, 2539–2544.
31. Kobayashi, K., Niikura, K., Takeuchi, C., Sekiguchi, S., Ninomiya, T., Hagiwara, K., Mitomo, H., Ito, Y., Osada, Y., Ijro, K. (2014) Enhanced Cellular Uptake of Amphiphilic Gold Nanoparticles with Ester Functionality. *Chem. Commun.* 50, 1265–1267.
32. Verma, A., Uzun, O., Hu, Y., Hu, Y., Han, H.-S., Watson, N., Chen, S., Irvine, D. J., Stellacci, F. (2008) Surface-Structure-Regulated Cell-Membrane Penetration by Monolayer-Protected Nanoparticles *Nature Mater.* 7, 588–595.

33. van Lehn, R. C., Atukorale, P. U., Carney, R. P., Yang, Y.-S., Stellacci, F., Irvine, D. J., Alexander-Katz, A. (2013) Effect of Particle Diameter and Surface Composition on the Spontaneous Fusion of Monolayer-Protected Gold Nanoparticles with Lipid Bilayers. *Nano Lett.* 13, 4060–4067.
34. van Lehn, R. C., Alexander-Katz, A. (2014) Free energy Change for Insertion of Charged, Monolayer-Protected Nanoparticles into Lipid Bilayers. *Soft Matter* 10, 648–658.
35. Sabella, S., Carney, R. P., Brunetti, V., Malvindi, M. A., Al-Juffali, N., Vecchio, G., Janes, S. M., Bakr, O. M., Cingolani, R., Stellacci, F., *et al.* (2014) A General Mechanism for Intracellular Toxicity of Metal-Containing Nanoparticles. *Nanoscale* 6, 7052–7061.
36. Uzun, O., Hu, Y., Verma, A., Chen, S., Centrone, A., Stellacci, F. (2008) Water-Soluble Amphiphilic Gold Nanoparticles with Structured Ligand Shells. *Chem. Commun.* 196-198.
37. In the nanoparticles designation **F8** stands for the thiolate derived from thiol **HF8** and **MUS** stands for the thiolate derived from thiol **HMUS**, all of the nanoparticles in the text are named accordingly.
38. Şologan, M., Cantarutti, C., Bidoggia, S., Polizzi, S., Pengo, P., Pasquato, L. (2016) Routes to the Preparation of Mixed Monolayers of Fluorinated and Hydrogenated Alkanethiolates Grafted on the Surface of Gold Nanoparticles. *Faraday Discuss.* 191, 527 – 543.
39. Stewart, A., Zheng, S., McCourt, M. R., Bell, S. E. J. (2012) Controlling Assembly of Mixed Thiol Monolayers on Silver Nanoparticles to Tune Their Surface Properties. *ACS Nano* 6, 3718–3726.
40. Gentilini, C., Evangelista, F., Rudolf, P., Franchi, P., Lucarini, M., Pasquato, L. (2008) Water-Soluble Gold Nanoparticles Protected by Fluorinated Amphiphilic Thiolates. *J. Am. Chem. Soc.* 130, 15678–15682.
41. Pengo, P., Polizzi, S., Battagliarin, M., Pasquato, L., Scrimin, P. (2003) Synthesis, Characterization and Properties of Water-Soluble Gold Nanoparticles with Tunable Core Size. *J. Mater. Chem.* 13, 2471-2478.
42. Andreozzi, P., Martinelli, C., Carney, R. P., Carney, T. M., Stellacci, F. (2013) Erythrocyte Incubation as a Method for Free-Dye Presence Determination in Fluorescently Labeled Nanoparticles. *Mol. Pharm.* 10, 875–882.
43. Arvizo, R. R., Miranda, O. R., Thompson, M. A., Pabelick, C. M., Bhattacharya, R., Robertson, J. D., Rotello, V. M., Prakash, Y. S., Mukherjee, P. (2010) Effect of Nanoparticle Surface Charge at the Plasma Membrane and Beyond. *Nano Lett.* 10, 2543–2548.
44. Nativo, P., Prior, I. A., Brust, M. (2008) Uptake and Intracellular Fate of Surface-Modified Gold Nanoparticles. *ACS Nano* 2, 1639–1644.

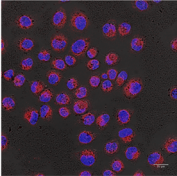
45. Lin, J., Alexander-Katz, A. (2013) Cell Membranes Open “Doors” for Cationic Nanoparticles/Biomolecules: Insights into Uptake Kinetics. *ACS Nano* 7, 10799–10808.
46. Heikkila, E., Martinez-Seara, H., Gurtovenko, A. A., Javanainen, M., Häkkinen, H., Vattulainen, I., Akola, J. (2014) Cationic Au Nanoparticle Binding with Plasma Membrane-like Lipid Bilayers: Potential Mechanism for Spontaneous Permeation to Cells Revealed by Atomistic Simulations. *J. Phys. Chem. C* 118, 11131 – 11141.
47. Goodman, C. M., McCusker, C. D., Yilmaz, T., Rotello, V. M. (2004) Toxicity of Gold Nanoparticles Functionalized with Cationic and Anionic Side Chains. *Bioconjugate Chem.* 15, 897–900.

TOC graphics

Charged H-/F- Mixed Monolayer Gold Nanoparticles



Easy Uptake



Toxicity analysis

